American Journal of Mechanical Engineering, 2018, Vol. 6, No. 3, 132-147
Available online at http://pubs.sciepub.com/ajme/6/3/6
©Science and Education Publishing
DOI:10.12691/ajme-6-3-6

Experimental Investigation of Wire-EDM Process Parameters for Surface Roughness in the Machining of Carbon Steel 1017 and Aluminum Alloy 6060

Mohammad S. Alsoufi*, Dhia K. Suker

Department of Mechanical Engineering, College of Engineering and Islamic Architecture, Umm Al-Qura University, Makkah, KSA
*Corresponding author: mssoufi@uqu.edu.sa

Received October 12, 2018; Revised November 17, 2018; Accepted November 28, 2018

Abstract Electrical discharge machining is an old technology that has been used for old manufacturing processes. Nowadays, the modernized version of the machine is used to manufacture different objects using a wire feed. The parameters in which the machine operates have diverse effects on product quality and surface finish. This paper investigates the performance of a wire electrical discharge machining process for different wire feed rates. The process is a non-traditional machining method. Several tests have been performed considering a carbon steel 1017 and aluminum alloy 6060 machined via Wire-EDM. By using different wire feed rates (3 mm/min, 5 mm/min and 7 mm/min), the average surface roughness, R_a, has been investigated in this study. Results show that the wire feed rate is a significant variable to the surface quality finish. The surface roughness of the test target materials increased as this variable increased. The present study recommends setting the wire feed rate as low as possible with the aim of improving results in the surface quality finish. The obtained results and some of the most necessary parameters affecting the manufacturing process of wire-EDM are briefly defined and are then discussed in detail in this study.

Keywords: *Wire-EDM, Surface Roughness, wire feed rate, carbon steel 1017, aluminum alloy 6060*

Cite This Article: Mohammad S. Alsoufi, and Dhia K. Suker, "Experimental Investigation of Wire-EDM Process Parameters for Surface Roughness in the Machining of Carbon Steel 1017 and Aluminum Alloy 6060." *American Journal of Mechanical Engineering*, vol. 6, no. 3 (2018): 132-147. doi: 10.12691/ajme-6-3-6.

1. Introduction

Historically, the first electrical discharge machining (EDM) application was based on old technology that utilized controlled electrical discharges to remove broken taps and drills metal. The machine was originally developed by Russian scientists during WWII in the Technical Institute of Moscow [1,2]. The essentials of EDM application can be traced back as far as 1770 when the English chemist Joseph Priestly discovered the erosive effect of electrical discharges or sparks. Nevertheless, it was not until 1943 at Moscow University when scientists exploited the destructive properties of electrical discharges in the manufacturing process [3,4]. Since that initial introduction to the manufacturing industry in the late 1940s, the EDM technique (an unconventional process) has become one of the preferred manufacturing methods used in machining materials as it does not require tools and there is no direct contact with the sample being manufactured [5].

Currently, in modern manufacturing industries, wire-EDM is defined as a technique of manufacturing involving 1D, 2D and 3D physical objects by a thin wire (0.1 to 0.3 mm diameter) eroding the material from a material which is a good conductor or semiconductor of electricity [6], for instance metals, metallic alloys, graphite, or even some ceramic materials [7,8]. The material removal during thin wire-EDM process takes place using the etching process, which removes materials form the workpiece, and flushing the debris using saline liquid [9,10,11]. The etching process occurs when the discharge current passes through the narrow gap between the electrode and the workpiece [12]. Generally, the conductor or semiconductor material is mounted on a computer numerical controlled (CNC) worktable. The gap between the target workpiece and the thin wire is around 0.025 to 0.05 mm and is maintained constant by a computer-controlled positioning system during the operation. The thin wire is continuously fed through the target workpiece by a microprocessor, which enables the machining of complex physical shapes [6,13].

Wire-EDM is an essential non-conventional machining process (thermo-electrical process), which is widely used in the aerospace [14,15], ordnance [16], automobile [17] and general engineering industries [13], because of a series of merits, such as workpieces with a wide range of hardness, the fact that there is no macro-mechanical force during the process, its high degree of precision, and so on [18,19]. The most significant benefit of the wire-EDM is its independence of the machined material's mechanical properties and its independence from the cutting force. So, conductive materials that are characterized by brittleness, high hardness, and strength that are "difficult-to-cut" can

be machined easily to the desired shape [20]. The quality and cutting efficiency in wire-EDM depends on the material to be used, and the process parameters used [13].

2. Experimental Details

2.1. Workpiece Design and Materials

Carbon steel 1017 and aluminum alloy 6060 have been used as a workpiece material in this research work, and it has application in a great many modern manufacturing industries. The shape of the workpiece materials of carbon steel 1017 and aluminum alloy 6060 is a rectangular block which has been cut into a total of four small pieces of 20 mm thickness each. The specification of each piece is 60 mm × 25 mm × 30 mm (length, width, and height, respectively) in the rectangular shape as illustrated in Figure 1. The chemical composition of carbon steel 1017 and aluminum alloy 6060 were analyzed using PMI-MASTER Pro2 and are provided in Table 1 and Table 2, respectively. All workpieces are initially cleaned before experimenting.

It is of the utmost significance before starting the experiments to clean the specimens of any surface contaminants, such as dust, grease, or any other soluble organic particles so that there will be no adverse effect on the results. To achieve this, all specimens were ultrasonically cleaned with organic solvents (ethyl alcohol) for 15 minutes followed by warm drying air. After cleaning, the specimens were stored for 24 hours until testing to allow the sample surface condition to equilibrate with the environment. This procedure is considered adequate at this stage.

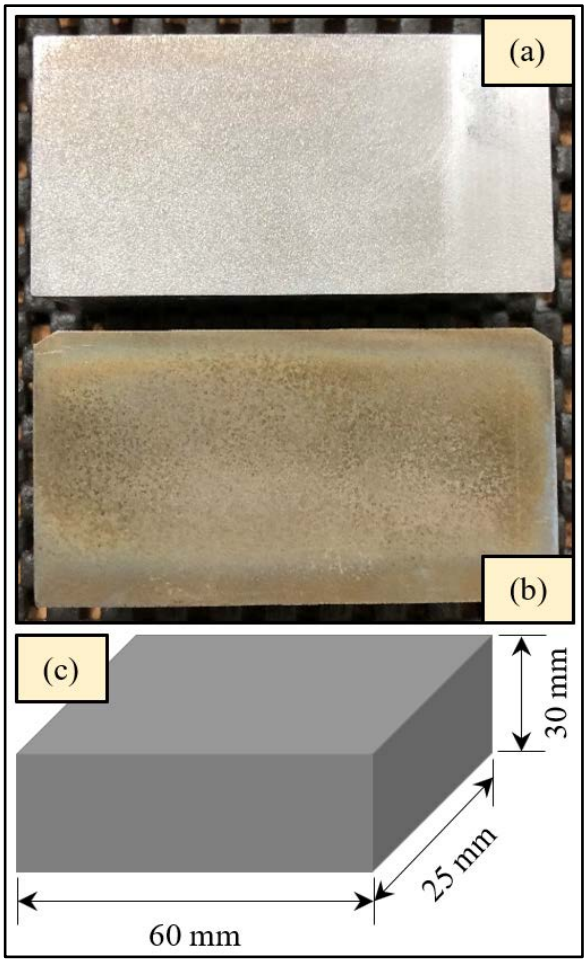

Figure 1. Photo of the (a) aluminum alloy 6060, (b) carbon steel 1017 and (c) 3D schematic object

Table 1. Chemical composition of carbon steel 1017

Elements	Fe	C	Si	Mn	Cr	Mo	Ni	Al	Co	Cu	Nb	Ti	V	W	Pb	Zr
Composition %	98.4	0.185	0.196	0.565	0.136	0.0263	0.0690	0.0084	0.0066	0.213	0.0096	0.0043	0.0058	0.0650	0.0750	0.0096

Table 2. Chemical composition of aluminum alloy 6060

Elements	Al	Si	Fe	Cu	Mn	Mg	Zn	Cr	Ni	Ti	Be	Ca	Pb	Sn
Composition %	98.5	0.435	0.183	0.0094	0.0256	0.616	0.0768	0.0026	0.0198	0.0120	0.0010	0.0026	0.0167	0.0141
Elements	**Sr**	**V**	**Bi**	**Zr**	**B**	**Ga**	**Cd**	**Co**	**Ag**	**In**	**Ce**	**Hg**	**La**	
Composition %	0.0010	0.0033	0.0401	0.0024	0.0078	0.0151	0.0030	0.0020	0.0058	0.0073	0.0151	0.0050	0.0061	

Table 3. Main properties of the thin brass electrode

Electrode Material	Thermal Conductivity (W/m*K)	Melting Point (K)	Electrical Resistivity (Ω cm)	Specific Heat Capacity (J/g °C)
Brass	159	990	4.7	0.38

2.3. Machining Method and Procedure

A commercial precision AgieCharmilles wire electrical discharge machine wire-EDM (purchased from GF Machining Solutions, USA) has been used to conduct the experiments. This consists of a machine tool, a power supply unit and a flushing unit. In the wire-EDM cutting machine, all three axes with a repeatable positioning accuracy of 1 µm and 0.1 µm resolution, are a closed-loop servo-controlled testing machine and can be programmed to follow computer numerical control (CNC) G-code routines which are fed by the control board. AC brass (CuZn37), 500 thin wire electrode of 0.25 mm diameter, has been used (costing about ~20 $/kg) with a total resistance of 500 N/mm^2, 20% elongation, 25% IACS conductivity and taking deionized water (costing about ~200 $ for 45 litter/machine and ~500 hours lifetime) as the dielectric fluid (electrically non-conducting), which also acts as a coolant and flushes the debris away. AC brass 500 thin wire electrode is made from a very pure alloy in order to guarantee consistent quality and performance for conic machining. Diamond guides are usually expensive to replace but last a long time. The thin brass wire was selected due to its properties that are suitable for high sparking energy machining. The thin brass wire travels through the target workpiece material from upper and lower thin wire guides. Once the brass wire is wound onto the wire drum, that amount of wire is used for all the experiments of each material and is replaced once the target material is changed in order to avoid wear phenomenon. Work material is tightly clamped onto the worktable to avoid any relative motion between the wire and the material. Constant dielectric flow is ensured during the experimentation. The main properties of the electrode characteristics used in in this experiment are listed in Table 3.

Typically, the cutting procedure occurs while the target workpiece material is submerged in deionized fluid, which aids in cooling down the procedure and flushing away the cut target material. It therefore leaves the target material with a smooth surface profile that often requires no further polishing or even finishing. It is worth mentioning that the thin cutting wire should not touch the conductive or semi-conductive material and that the cutting itself is due to the erosion that occurs when a spark forms between the thin cutting wire and the raw material.

The fundamental principle behind the wire-EDM process is a sequence of electric sparks created due to passing high current between the material and the thin wire electrode. The electrical discharging process generates dramatic heat causing melting and evaporation in the local surface layers on both target material sides and the electrode. In addition, the heat causes vaporization of the dielectric fluid and generates high-pressure waves, which wash out the molten and vaporized metal into small pieces from the target material. The fluid then carries the droplets of metal away.

2.4. Determination of Machining Parameters

The machining process parameters have a significant influence on the wire-EDM performance. According to the operating experience, machine limits and some preliminary tests, the basic machine setting parameters are shown in Table 4, in which there was no breakage of wire electrode throughout the process due to dynamic spark energy in the wire-EDM.

There have been a great many publications regarding the quality of the surface finish achieved by wire-EDM. The influences of some machining process parameters such as pulsed current [2,21-28], pulse-on time [21-25,27,28], pulse-off time [21,24,28], gap voltage [23,24,28], dielectric liquid pressure [23,25,27,29] and electrode material [30] have been thoroughly investigated. However, when seeking information about the effect of the wire feed rate on the surface roughness using wire-EDM, we found no authoritative public data available. Therefore, the influence of the wire feed rate was investigated and required close attention in this research with three different levels of each parameter while other parameters kept constant.

Table 4. Process parameters with their values at three levels

Parameters	Symbol	Unit	Level 1	Level 2	Level 2
Gap Voltage	*V*	Volt	40		
Peak Current	*PC*	A	10		
Pulse-on Time	T_{on}	µm	6		
Pulse-off Time	T_{off}	µm	12		
Wire Feed Rate	*WFR*	mm/min	3	5	7
Wire Tension	*WT*	N	11		
Wire Size	*WS*	Mm	0.25		
Wire Material	*WM*	-	Brass Wire		
Dielectric	-	-	Deionized Water		
Polarity	-	-	Wire electrode: a negative polarity Workpiece: a positive polarity		
Environment Temperature	ET	℃	20±1		
Environment Humidity	EH	%	40±5		

Some of the most necessary parameters affecting the manufacturing process of wire-EDM are briefly defined as follows [1,8,23,31,32]:

- **Discharge Current:** this is the value of the current applied to the electrode during the pulse-on time in the wire-EDM. The discharge current is one of the critical input process parameters of the wire-EDM together with discharge duration and relatively constant voltage for a given tool and target workpiece materials.
- **Peak Current:** this is the amount of power used in discharge machining. During each pulse-on time, the current increases until it reaches a preset level, which is expressed as the peak current. In wire-EDM processes, the peak current is the surface area of the cut which governs the maximum amount of amperage. Higher current is used in roughing operations and in creating cavities or details with large surface areas. Higher currents will improve the material removal rate (MRR) but then again reduce the surface roughness, R_a.
- **Servo Voltage:** this acts as the reference voltage to control the wire advances and retractions. It is also

called a spark gap set voltage which refers to the actual gap between the workpiece and the wire electrode used for cutting. When the mean applied voltage is higher than the set servo voltage level, the thin wire advances. In contrast, if the mean applied voltage is lower than the set servo voltage level, then, the thin wire retracts. When a smaller value of servo voltage is set, the mean gap becomes thinner, which leads to a rise in some electric sparks, resulting in a higher machining rate. Nevertheless, the state of machining at the gap might become unstable, causing thin wire breakage.

- **Gap Voltage:** this is voltage applied between the electrode and the target workpiece during the wire-EDM. The greater the gap voltage, the more significant will be the electric discharge. If the gap voltage rises, the peak current will also rise. The open gap voltage is the voltage read across the electrode and workpiece space before the spark. In some wire-EDM machines, each of these factors shows machining voltage.
- **Pulse-on Time:** this is the time in microseconds (μs) for which the current is applied to the electrode during each wire-EDM cycle. The conductive material removed is directly proportional to the quantity of energy applied during the pulse-on time. The current and the pulse-on time control this energy. The higher the pulse-on time, the higher will be the energy applied, thereby generating a greater amount of heat energy during this period. MRR depends upon the total amount of energy applied during the pulse-on time. MRR depends on a longer or shorter pulse period. Longer pulse duration improves the MRR of debris from the machined area.
- **Pulse-off Time:** this represents the duration of time between the two simultaneous sparks, and is also expressed in microseconds (μs), which is the time between discharges. Pulse-off time does not affect discharge energy. Pulse-off time is the pause between discharges that allows the debris to solidify and be flushed away by the dielectric before the next discharge. With a lower value of pulse-off time, there are some discharges in a given time, increasing the efficiency of the sparking. Consequently, the cutting rate also rises. However, reducing pulse-off time can overload the thin wire, causing thin wire breakage and instability of the cut by not permitting sufficient time to evacuate the debris before the next discharge.
- **Wire Feed Rate:** this is the feed rate at which the wire electrode travels along the thin wire guide path and is fed continuously for sparking. In wire-EDM, wire electrode occupies almost 70% of the machining cost. Therefore, it is required to set a low wire feed rate where stable machining with no wire breakage occurs. As the wire feed rate rises, the consumption of thin wire along with the cost of machining will increase. Low wire speed will cause thin wire breakage at high cutting speed.
- **Wire Tension:** it is important to keep the wire tension high enough such that the wire stays straight otherwise the wire will be drawn behind. Within the range under consideration, an increase in wire tension significantly raises both the accuracy and the cutting speed. The higher tension reduces the wire vibration amplitude and hence decreases the cut width with the purpose of the speed increasing for the same discharge energy. Nevertheless, if the applied wire tension exceeds the tensile strength of the thin wire, it leads to thin wire breakage.
- **Dielectric Flow Rate:** this is the rate at which the dielectric fluid is circulated. Flushing is significant for effective machining. Flushing pressure is produced from the top and bottom nozzles. The high flow rate of the dielectric fluid is necessary for machining with high pulse power and also applies to cutting a thicker workpiece. Low input pressure is used for the thin workpiece dielectric fluid flow rate.
- **Duty Cycle:** this is a percentage of the pulse-on time relative to the total cycle time.

2.5. Measuring Method

There are various surface roughness amplitude parameters used in industry, such as average roughness, R_a, root mean square, R_q, ten-point height, R_z, total profile depth, R_t, skewness, R_{sk}, kurtosis, R_{ku}, and so on. The most frequently-used surface roughness amplitude parameter applied to the evaluation of machined surface materials is the amplitude parameter, R_a, and it is becoming the universally recognized one. In this research paper, the average roughness, R_a, is considered here and is defined as the area between the average surface roughness profile and its mean line or the integral with the real absolute value of the average surface roughness profile height over the assessment length. Therefore, the average roughness, R_a, is defined by the following equation:

$$R_a = \frac{1}{L}\int_0^L \left|Y(x)\right| dx \tag{1}$$

where R_a is the arithmetic average deviation from the mean line, L the sampling length and Y is the ordinate distribution of the profile curve (peak-to-valley). The average surface roughness amplitude parameter, R_a, was selected according to the recommendations in the literature review and with consideration of the data processing facilities available with differing levels of information [33-37].

There are several ways of measuring average surface roughness, R_a, such as image processing, microscopes, contact and non-contact stylus type instruments, a profile tracing instrument, and so on. A conventional contact-type Taly-Surf® profilometer from Taylor Hobson Precision, Inc. was used with a contact force of 0.7 mN, displacement sensitivity of 50 nm and tip radius of a 2 μm. The experiments were performed under wear-free and high-precision position measurement, which can offer a high degree pf precision of up to 0.8 nm, a measuring range (x-axis) of 12.5 mm, and linear speed up to 0.5 mm/s. The traces were auto-leveled, set up to a linear least-squares (LLS) straight line and then filtered with a standard low-pass of 0.8 mm cut-off wavelength and filter CR ISO. Details of the average surface roughness measurements procedure and calibration trials have been reported

elsewhere [38-51]. In general, the calibration results showed that the cantilever beam system (stylus with beam) at only one end was a linear mass-spring system (R^2 > 0.999) under operational and environmental conditions, generally at 20°C ± 1°C temperature and 40% ± 5% relative humidity, with an absolute uncertainties value of < 1% and measurement resolution down to at worst 50 nm. The obtained results were revised and analyzed qualitatively with Origin Lab® 2018 software. Figure 2 shows the measuring technique of the carbon steel 1017 (Fe = 98.4%) and aluminum alloy 6060 (Al = 98.5%).

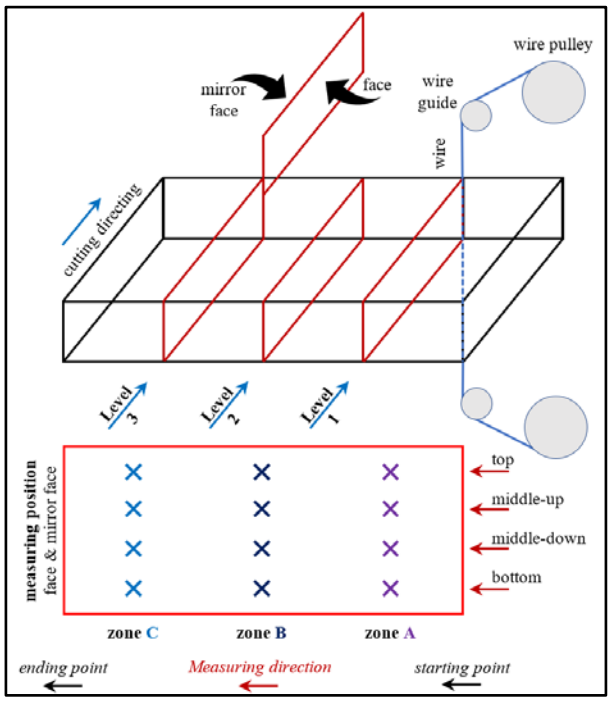

Figure 2. Schematic diagram of the sample design and measuring technique

3. Experimental Results and Discussion

According to the experimental set-up and process parameters setting shown in Figure 2 and Table 3, the average surface roughness, R_a, was measured and plotted using OriginLab® 2018 software. Bear in mind that only wire feed rate was set as a variable process parameter (3 mm/min, 5 mm/min and 7 mm/min) while other parameters were kept constant (gap voltage, pulse-on time, pulse-off time, wire tension, wire size, wire material and dielectric). The first part of the experimental study was conducted for machined workpiece surface roughness profile performance of the carbon steel 1017 (Fe = 98.4%) and aluminum alloy 6060 (Al = 98.5%) (see subsection 3.1), the second part of the experimental study was carried out for machined workpiece surface roughness finish quality performance of the carbon steel 1017 (see subsection 3.2) and the third part of the experimental study was carried out for machined workpiece surface roughness finish quality performance of the aluminum alloy 6060 (see subsection 3.3).

3.1. Surface Roughness Profile Performance

Figure 3 and Figure 4 show the significantly different conditions in the surface roughness behavior profiles of machined materials over a 10 mm measuring distance. Both Figure 3(a) and Figure 4(a) show the frequent peaks-to-valleys distribution with narrower and smaller wider peaks-to-valleys indicating that the wire-EDM process parameters controlled the cut face and mirror cut face. The machined cut face follows a new pattern regardless of the value of R_a indicating that wire-EDM procedure plays a significant role in changing the overall peaks-to-valleys profiles. The data generated from Figure 3(a) reveal that the surface behavior distribution region of the carbon steel 1017 is smooth, −7.711 µm < surface profile < +6.174 µm, whereas, the data generated from Figure 4(a) reveal that the surface behavior distribution region of the aluminum alloy 6060 is rough, −13.741 µm < surface profile < +11.862 µm. The data generated from Figure 3(b) and Figure 4(b) show the histograms of the distribution of vertices and upgrades located on the machined samples. The distribution profile of both samples (carbon steel 1017 and aluminum alloy 6060) is characterized by a significant natural fluctuation of changes in the value of *R*-family parameters and more significantly changed the values of these parameters. Surprisingly, the R_a of aluminum alloy 6060 (Al = 98.5%) was almost three times rougher than that of carbon steel 1017 (Fe = 98.4%), which is more consistent with the mechanical properties of both target materials. Notice that all three levels of process parameters show uniform profile distribution for both carbon steel 1017 and aluminum alloy 6060.

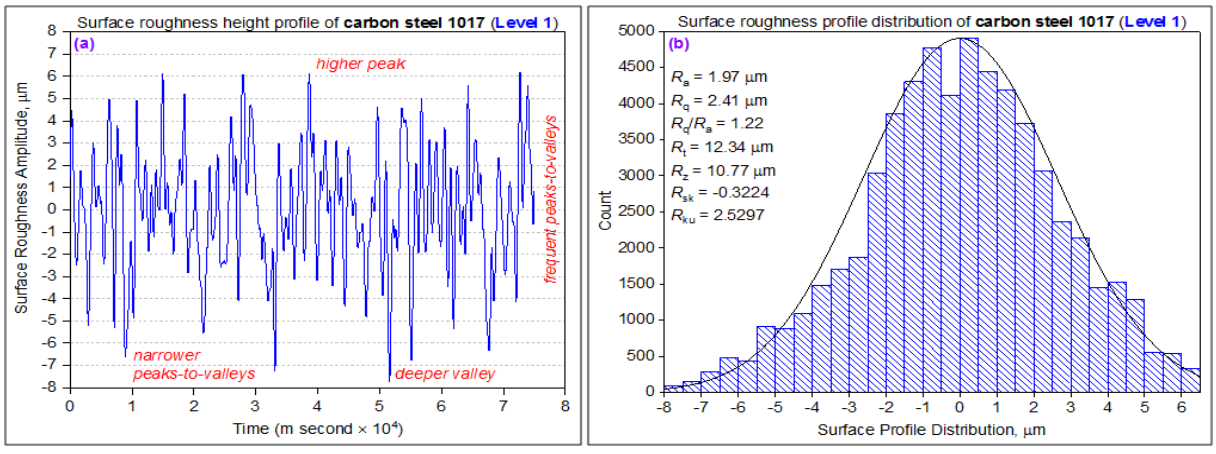

Figure 3. Surface roughness profile of carbon steel 1017 (a) height profile and (b) distribution profile

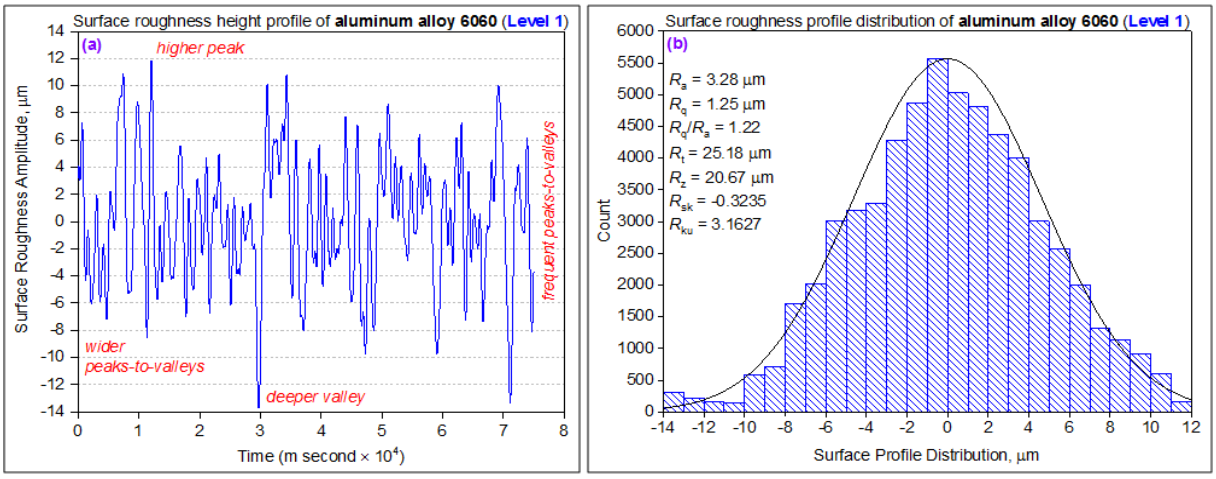

Figure 4. Surface roughness profile of aluminum alloy 6060 (a) height profile and (b) distribution profile

The profile roughness parameter ratio R_q/R_a performance (root means square, R_q, to average surface roughness, R_a) tends to follow the similar periodic trend of about ~1.2±0.03 with only less than ~2% difference.

Figure 3(b) and Figure 4(b) provide the general trend of the third-order and fourth-order central moments of skewness, R_{sk}, (3^{rd} moment) and kurtosis, R_{ku}, (4^{th} moment). Skewness, R_{sk}, (3^{rd} moment) is defined by ISO 4287 (1997) [52] as it evaluates the degree of asymmetry distribution and is categorized as positive skewness (surfaces are 'empty' of material) or negative skewness (surfaces are 'full' of material). This is a significant process parameter for tribological applications, such as friction, wear and lubrication. A Gaussian distribution presents R_{sk} = 0 whereas kurtosis, R_{ku}, (4^{th} moment) is defined by ISO 4287 (1997) [52] as it evaluates the distribution sharpness with R_{ku} = 3 for the normal distribution. The surface profile is dominated by sharp peaks (spiky wave) when R_{ku} > 3, whereas the surface is dominated by bumpy peaks when R_{ku} < 3. It can be concluded that the general trend is a negatively skewed distribution for skewness, R_{sk}, (3^{rd} moment) for both machined samples (carbon steel 1017 and aluminum alloy 6060). However, it shows 100% leptokurtic, homogeneous and narrow scatter with a high degree of peakedness for the kurtosis, R_{ku}, (4^{th} moment) for carbon steel 1017 (Fe = 98.4%), while it shows 100% platykurtic distribution, heterogeneous, little wider scatter and peaks are bumpy with a low degree of peakedness for the kurtosis, R_{ku}, (4^{th} moment) for aluminum alloy 6060 (Al = 98.5%).

3.2. Carbon Steel 1017 Performance

Figure 5(a), Figure 5(b) and Figure 5(c) show unpredicted behavior of the surface roughness performance of carbon steel 1017 cut by thin brass wire-EDM at level 1 process parameters (WFR = 3 mm/min) and measured at three different zones (A, B and C) and four different sub-zones (A1, A2, A3 and A4), (B1, B2, B3 and B4) and (C1, C2, C3 and C4) for both cut face and mirror cut face.

At level 1 (3 mm/min wire feed rate) and zone A, as shown in Figure 5(a), the surface roughness values of the cut face were increased from 1.87 µm (at the top area, sub-zone A1) until it reached 2.25 µm (at the bottom area, sub-zone A4), where the cutting has been done by a lateral cross-section of the target material whereas, the surface roughness values of the mirror cut face were increased from 1.95 µm (at the top area, sub-zone A1) until it reached 2.36 µm (at the middle-down area, sub-zone A3) and then decreased to 2.15 µm. This behavior indicates that there are some differences between the cut face and the mirror cut face by almost ~0.04 µm implying smoother surface roughness in the former, although the same brass wire-EDM cutting method was used. This fluctuated in R_a due to wear phenomenon during the process cutting in contact between the thin wire brass and target material.

At level 1 (3 mm/min wire feed rate) and zone B, as shown in Figure 5(b), the surface roughness values of the cut face were increased from 1.97 µm (at the top area, sub-zone A1) until they reached 2.33 µm (at the middle-up and middle-down areas, sub-zones B2 and B3), where the cutting has been done by a lateral cross-section of the target material. After that, the R_a starts to improve by almost ~2.07 µm (at the bottom are, sub-zone B4) whereas, the surface roughness values of the mirror cut face were increased from 1.63 µm (at the top area, sub-zone B1) until they reached 2.22 µm (at the middle-up area, sub-zone B2) and then decreased to 2.1 µm. This behavior indicates that there are some differences between the cut face and mirror cut face by almost ~0.14 µm implying smoother surface roughness in the latter, although the same brass wire-EDM cutting method was used. It is also worth mentioning that the cut face and mirror cut face follow the same behavior and same trend of peaks and valleys unlike zone A performance.

At level 1 (3 mm/min wire feed rate) and zone C, as shown in Figure 5(c), the surface roughness values of the cut face were increased from 1.79 µm (at the top area, sub-zone C1) until it reached 2.11 µm (at the bottom area, sub-zone C4), where the cutting has been done by a lateral cross-section of the target material whereas, the surface roughness values of the mirror cut face started at 2.03 µm (at the top area, sub-zone C1) until it reached 2.3 µm (at the middle-up area, sub-zone C2) and then decreased to 1.94 µm. This behavior indicates that there are some differences between the cut face and mirror cut face by almost ~0.17 µm implying smoother surface roughness in the former, although the same brass wire-EDM cutting method was used. Also, it is worth mentioning that the cut

face and mirror cut face show some irregularity of distribution between peaks and valleys unlike zone B performance. During machining of carbon steel 1017 using a brass electrode the factors result in the maximum wear ratio causing irregularity surface roughness distribution, but the wear cannot be avoided entirely. Nevertheless, to achieve the high surface finish quality, the wear has to be compensated for by the electrode's renewal. This phenomenon governs tool wear characteristics either by erosion of electrode material and/or by deposition of workpiece material on the tool electrode. Besides, the surface roughness behavior at sub-zone C2 (for mirror cut face) shows very rough area ($R_a \approx 2.3$ µm) due to penetrating micro-cracks or scratches in the sub-surface.

Figure 5(d) shows the mean and standard deviation (mean±SD) values of the carbon steel 1017 cut by wire-EDM including the cut face and mirror cut face at level 1 of the process parameters (WFR = 3 mm/min). As can be seen, the mean±SD values at level 1 (zone A) were 2.09±0.17 µm (for cut face) and 2.13±0.17 µm (for mirror cut face) indicating that 2% increased for the mirror cut face compared to cut face at the same spot of measurement with the same standard deviation. The mean±SD values at level 1 (zone B) were 2.18±0.18 µm (for cut face) and 2.04±0.27 µm (for mirror cut face) indicating that 6% decreased for the mirror cut face compared to cut face at the same spot of measurement with 33% differences in the standard deviation. The mean±SD values at level 1 (zone C) were 1.9±0.14 µm (for cut face) and 2.07±0.15 µm (for mirror cut face) indicating that 8% increased for the mirror cut face compared to cut face at the same spot of measurement with 6% differences in the standard deviation. Roughly speaking, zone C (ending point) regardless of which subzones represents the smoothest average surface roughness compared with zone A (starting point) and zone B (middle point) due to stability of wire tension compared with the first impact at zone A.

Figure 6(a), Figure 6(b) and Figure 6(c) show unpredicted behavior of the surface roughness performance of carbon steel 1017 (Fe = 98.4%) cut by thin brass wire-EDM at level 2 process parameters (WFR = 5 mm/min) and measured at three different zones (A, B and C) and four different sub-zones (A1, A2, A3 and A4), (B1, B2, B3 and B4) and (C1, C2, C3 and C4) for both cut face and mirror cut face.

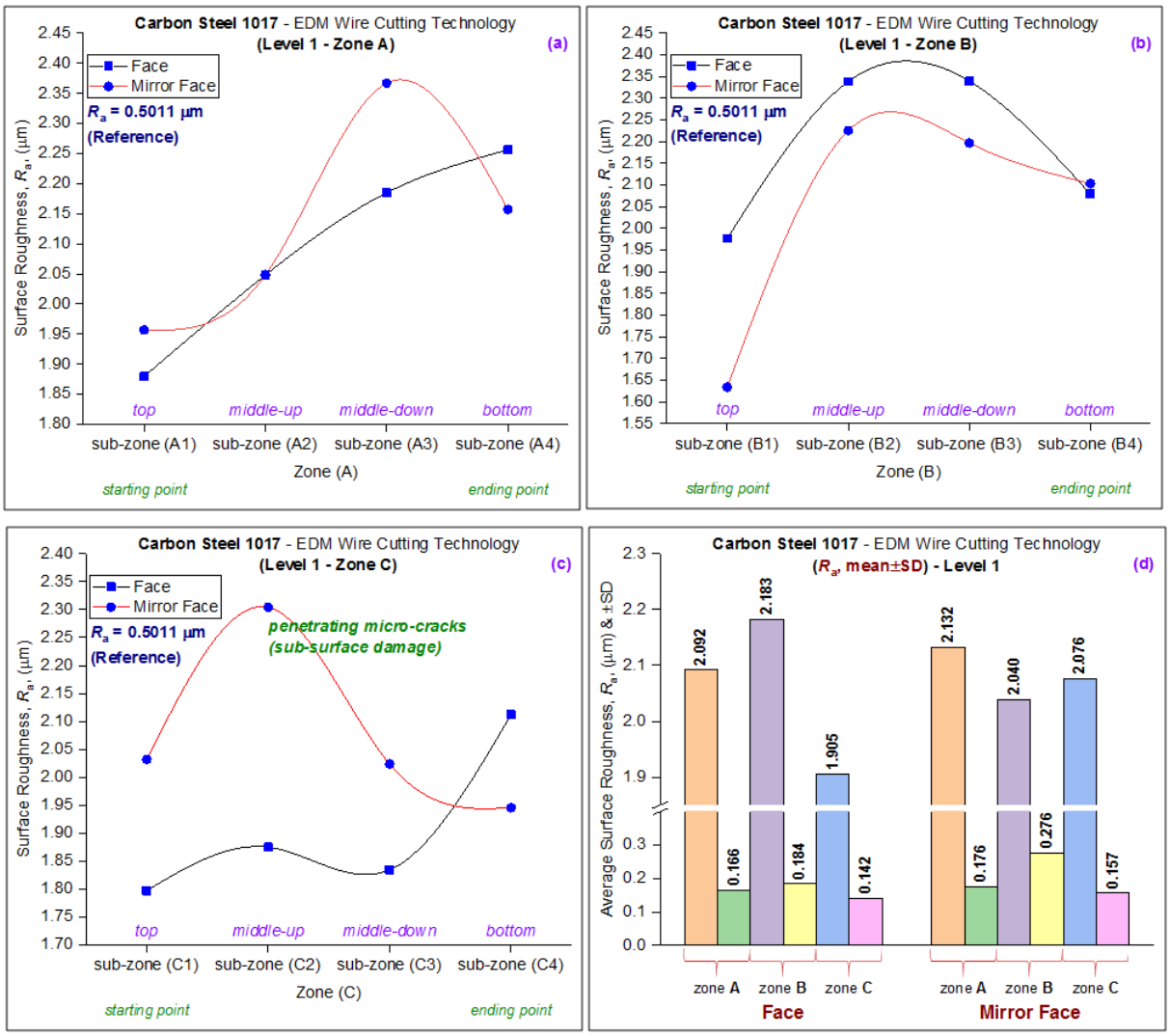

Figure 5. Surface roughness of carbon steel 1017 at level 1 parameters with different zones (a) zone A, (b) zone B, (c) zone C and (d) average surface roughness with a standard deviation

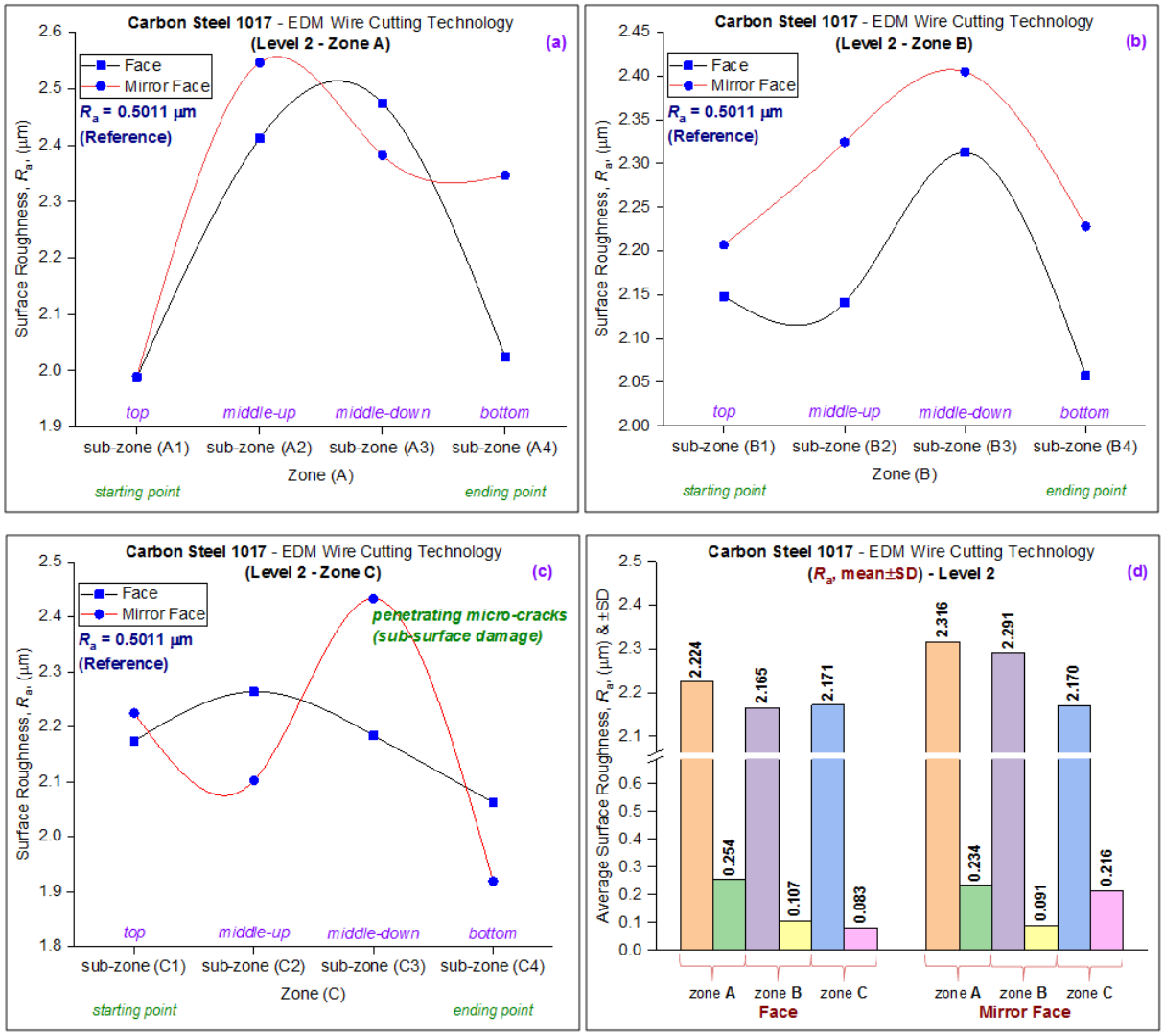

Figure 6. Surface roughness of carbon steel 1017 at level 2 parameters with different zones (a) zone A, (b) zone B, (c) zone C and (d) average surface roughness with a standard deviation

At level 2 (5 mm/min wire feed rate) and zone A, as shown in Figure 6(a), the surface roughness values of the cut face were increased from 1.98 µm (at the top area, sub-zone A1) until they reached 2.47 µm (at the middle-up area, sub-zone A2), where the cutting has been done by a lateral cross-section of the target material whereas, the surface roughness values of the mirror cut face were increased from 1.98 µm (at the top area, sub-zone A1) until they reached 2.54 µm (at the middle-up area, sub-zone A2) and then decreased to 2.34 µm. This behavior indicates that there are some differences between the cut face and mirror cut face by almost ~0.09 µm implying smoother surface roughness in the former, although the same brass wire-EDM cutting method was used.

At level 2 (5 mm/min wire feed rate) and zone B, as shown in Figure 6(b), the surface roughness values of the cut face were increased from 2.14 µm (at the top area, sub-zone A1) until it reached 2.31 µm (at the middle-down areas, sub-zones B3), where the cutting has been done by a lateral cross-section of the target material. After that, the R_a starts to improve by almost ~2.05 µm (at the bottom area, sub-zone B4) whereas, the surface roughness values of the mirror cut face were increased from 2.2 µm (at the top area, sub-zone B1) until they reached 2.4 µm (at the middle-down area, sub-zone B3) and then decreased to 2.22 µm. This behavior indicates that there are some differences between the cut face and mirror cut face by almost ~0.12 µm implying smoother surface roughness in the former as it is in zone A with rougher surface roughness by 25%, although the same brass wire-EDM cutting method was used. It is worth mentioning, in particular, that the cut face and mirror cut face follow the same behavior and same trend of peaks and valleys unlike zone A performance at subzone A4 where mirror cut face shows a slight improvement in R_a compared with a cut face.

At level 2 (5 mm/min wire feed rate) and zone C, as shown in Figure 6(c), the surface roughness values of the cut face were increased from 2.17 µm (at the top area, sub-zone C1) until it reached 2.26 µm (at the middle-up area, sub-zone C2), where the cutting has been done by a lateral cross-section of the target material whereas, the surface roughness values of the mirror cut face started at 2.22 µm (at the top area, sub-zone C1) until they reached 2.4 µm (at the middle-down area, sub-zone C3) and then decreased to 1.91 µm. This behavior indicates that there are some differences between the cut face and mirror cut face by almost ~0.0015 µm implying smoother surface roughness in the latter, although the same brass wire-EDM

cutting method was used. It is worth mentioning, in particular, the cut face and mirror cut face show some irregularity of distribution between peaks and valleys unlike zone B performance where no correlation between the two faces was observed. Besides, the surface roughness behavior at sub-zone C3 (for mirror cut face) shows a very rough area ($R_a \approx 2.4$ µm) due to penetrating micro-cracks or scratches in the sub-surface.

Figure 6(d) shows the mean and standard deviation (mean±SD) values of the carbon steel 1017 cut by wire-EDM including the cut face and mirror cut face at level 2 of the process parameters. As can be seen, the mean±SD values at level 2 (zone A) were 2.22±0.25 µm (for the cut face) and 2.31±0.23 µm (for the mirror cut face) indicating a 3% increased for the mirror cut face compared to cut face at the same spot of measurement with the same standard deviation. The mean±SD values at level 2 (zone B) were 2.16±0.1 µm (for the cut face) and 2.29±0.09 µm (for mirror cut face) indicating that 6% increased for the mirror cut face compared to cut face at the same spot of measurement with the 10% differences in the standard deviation. The mean±SD values at level 2 (zone C) were 2.17±0.08 µm (for cut face) and 2.16±0.21µm (for mirror cut face) indicate a 0.4% decrease for the mirror cut face compared to cut face at the same spot of measurement with the 61% differences in the standard deviation. Roughly speaking, zones B and C (middle point and ending point) represent the smoothest average surface roughness compared with zone A (starting point). Indeed, in wire-EDM, due to the instability of wire tension at the impact point (starting point), the R_a always represents high values compared to other zones and subzones.

Figure 7(a), Figure 7(b) and Figure 7(c) show unpredicted behavior of the surface roughness performance of carbon steel 1017 cut by thin brass wire-EDM at level 3 process parameters (WFR = 7 mm/min) and measured at three different zones (A, B and C) and four different sub-zones (A1, A2, A3 and A4), (B1, B2, B3 and B4) and (C1, C2, C3 and C4) for both cut face and mirror cut face.

At level 3 (7 mm/min wire feed rate) and zone A, as shown in Figure 7(a), the surface roughness values of the cut face were increased from 2.14 µm (at the top area, sub-zone A1) until they reached 2.41 µm (at the middle-down area, sub-zone A3), where the cutting has been done by a lateral cross-section of the target material whereas, the surface roughness values of the mirror cut face were increased from 1.84 µm (at the top area, sub-zone A1) until they reached 2.55 µm (at the middle-up area, sub-zone A2) and then decreased to 2.28 µm. This behavior indicates that there are some differences between the cut face and mirror cut face by almost ~0.03 µm implying smoother surface roughness in the former, although the same brass wire-EDM cutting method was used.

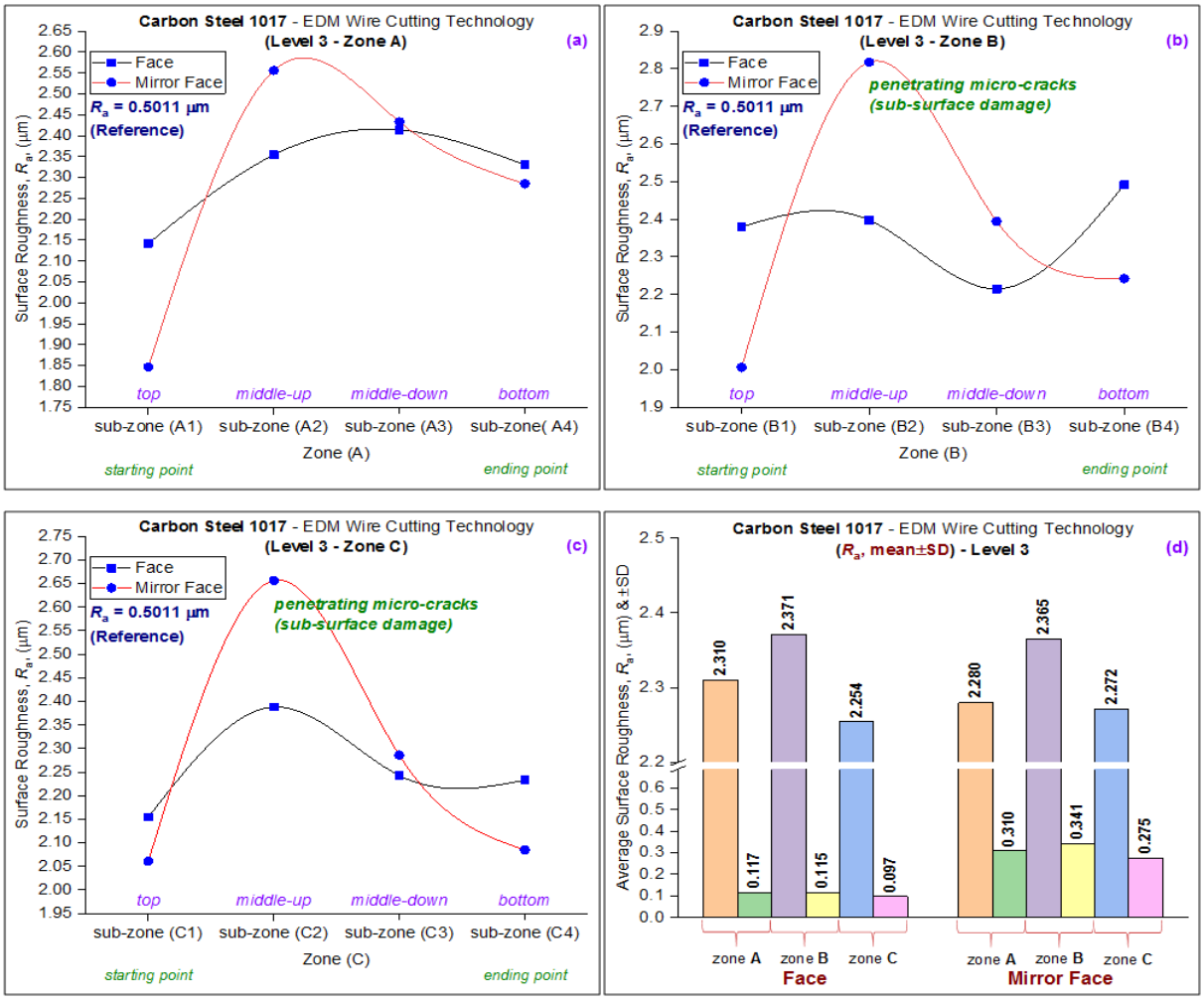

Figure 7. Surface roughness of carbon steel 1017 at level 3 parameters with different zones (a) zone A, (b) zone B, (c) zone C and (d) average surface roughness with a standard deviation

At level 3 (7 mm/min wire feed rate) and zone B, as shown in Figure 7(b), the surface roughness values of the cut face fluctuated all over zone B from 2.3 µm to 2.4 µm, where the cutting has been done by a lateral cross-section of the target material whereas, the surface roughness values of the mirror cut face were increased from 2 µm (at the top area, sub-zone B1) until they reached 2.8 µm (at the middle-up area, sub-zone B2) and then decreased to 2.24 µm. This behavior indicates that there are some differences between the cut face and mirror cut face by almost ~0.005 µm implying smoother surface roughness in the latter with rougher surface roughness by 83%, although the same brass wire-EDM cutting method was used. It is vital to mention that the cut face and mirror cut face follow the same behavior and same trend of peaks and valleys unlike their zone A performance. Besides, the surface roughness behavior at sub-zone B2 (for mirror cut face) shows very rough area ($R_a \approx 2.85$ µm) due to penetrating micro-cracks, spherical debris, recast layer, micro-voids or scratches in the sub-surface.

At level 3 (7 mm/min wire feed rate) and zone C, as shown in Figure 7(c), the surface roughness values of the cut face were increased from 2.15 µm (at the top area, sub-zone C1) until they reached 2.38 µm (at the middle-up area, sub-zone C2), where the cutting has been done by a lateral cross-section of the target material whereas, the surface roughness values of the mirror cut face started at 2.06 µm (at the top area, sub-zone C1) until they reached 2.65 µm (at the middle-up area, sub-zone C2) and then decreased to 2.08 µm. This behavior indicates that there are some differences between the cut face and mirror cut face by almost ~0.0017 µm implying smoother surface roughness in the former, although the same brass wire-EDM cutting method was used. It is vital to mention that the cut face and mirror cut face show some irregularity of distribution between peaks and valleys unlike zone A performance. Besides, the surface roughness behavior at sub-zone C3 (for mirror cut face) shows very rough area ($R_a \approx 2.65$ µm) due to penetrating micro-cracks or scratches in the sub-surface.

Figure 7(d) shows the mean and standard deviation (mean±SD) values of the carbon steel 1017 cut by wire-EDM including the cut face and mirror cut face at level 3 of the process parameters. As can be seen, the mean±SD values at level 3 (zone A) were 2.31±0.11 µm (for cut face) and 2.28±0.31 µm (for mirror cut face) indicating that 1% decreased for the mirror cut face compared to cut face at the same spot of measurement with the same standard deviation. The mean±SD values at level 3 (zone B) were 2.37±0.11 µm (for cut face) and 2.36±0.34 µm (for mirror cut face) indicating a 0.4% decrease for the mirror cut face compared to cut face at the same spot of measurement with the 67% differences in the standard deviation. The mean±SD values at level 3 (zone C) were 2.25±0.09 µm (for cut face) and 2.27±0.27 µm (for mirror cut face) indicating a 0.8% decrease for the mirror cut face compared to cut face at the same spot of measurement with 66% differences in the standard deviation. Roughly speaking, zone C (ending point) represents the smoothest average surface roughness compared with zones A and B (starting point and middle point).

In general, R_a decreased with a decrease in the wire feed rate and the best-achieved surface roughness was R_a = 1.63 µm at 3 mm/min wire feed rate. Another exciting observation in the data analysis is that there are no striations all over the carbon steel 1017 samples and smooth cutting behavior appears at the top spot area and then the R_a starts to fluctuate in the irregularity pattern. A possible reason for this feature would account for the flow of molten material during the discharge that significantly formed and recast on the cut surface. Such recast formation of the molten layer can subsequently fulfill some spark-induced cavities and other uneven features, thus decreasing the overall surface roughness. This explanation is also noted by Wang *et al.* [53] and Punturat *et al.* [54]. During Wire-EDM, high temperature of the parking zone (A, B, C) and sub-zones (A1, A2, A3, A4), (B1, B2, B3, B4) and (C1, C2, C3, C4) causes the target materials (carbon steel 1017, Fe = 98.4%) to melt during pulse-on time. During pulse-off time, part of the molten metal became solidified and quenched due to rapid cooling. Thermal residual stress produced due to such a rapid heating and cooling cycle results in the formation of surface cracks in the recast layer leading to high surface roughness finish.

3.3. Aluminum Alloy 6060 Performance

Generally, similar surface roughness finish quality results were noticed for aluminum alloy 6060 (Al = 98.5%) compared to carbon steel 1017 (Fe = 98.5%) when using thin brass wire-EDM. However, the surface finish quality of carbon steel 1017 was better when applying similar process parameter conditions.

Figure 8(a), Figure 8(b) and Figure 8(c) show unpredicted behavior of the surface roughness performance of aluminum alloy 6060 cut by brass wire-EDM at level 1 process parameters (WFR = 3 mm/min) and measured at three different zones (A, B and C) and four different sub-zones (A1, A2, A3 and A4), (B1, B2, B3 and B4) and (C1, C2, C3 and C4) for both cut face and mirror cut face.

At level 1 (3 mm/min wire feed rate) and zone A, as shown in Figure 8(a), the surface roughness values of the cut face were increased from 3.15 µm (at the top area, sub-zone A1) until they reached 3.81 µm (at the bottom area, sub-zone A4), where the cutting has been done by a lateral cross-section of the target material whereas, the surface roughness values of the mirror cut face were registered the low R_a at 3.65 µm (at the middle-up area, sub-zone A2) until it reached 4 µm (at the bottom area, sub-zone A4). This behavior indicates that there are some differences between the cut face and mirror cut face by almost ~0.44 µm implying smoother surface roughness in the former by 11.3%, although the same brass wire-EDM cutting method was used.

At level 1 (3 mm/min wire feed rate) and zone B, as shown in Figure 8(b), the surface roughness values of the cut face were increased from 3.28 µm (at the top area, sub-zone A1) until it reached 3.9 µm (at the middle-down area, sub-zone B3), where the cutting has been done by a lateral cross-section of the target material. After that, the R_a starts to improve by almost ~3.5 µm (at the bottom area, sub-zone B4) whereas, the surface roughness values of the mirror cut face were increased from 3.53 µm (at the top area, sub-zone B1) until they reached 4 µm (at the middle-down area, sub-zone B3) and then decreased to 3.59 µm.

This behavior indicates that there are some differences between the cut face and mirror cut face by almost ~0.13 µm implying smoother surface roughness in the former by 3.5%, although the same brass wire-EDM cutting method was used. It is worth mentioning here that the cut face and mirror cut face follow the same behavior and same trend of peaks and valleys unlike their zone A performance. Besides, the surface roughness behavior at sub-zone B3 (for both cut face and mirror cut face) shows a very rough area ($R_a \approx 3.9$ µm and 4.0 µm, respectively) due to penetrating micro-cracks or scratches in the sub-surface.

At level 1 (3 mm/min wire feed rate) and zone C, as shown in Figure 8(c), the surface roughness values of the cut face were increased from 3.28 µm (at the top area, sub-zone C1) until they reached 3.44 µm (at the middle-down area, sub-zone C3), where the cutting has been done by a lateral cross-section of the target material. In contrast, the surface roughness values of the mirror cut face started at 3.29 µm (at the top area, sub-zone C1) until they reached 4.26 µm (at the middle-down area, sub-zone C3) and then decreased to 3.6 µm. This behavior indicates that there are some differences between the cut face and mirror cut face by almost ~0.42 µm implying smoother surface roughness in the former by 11.3%, although the same brass wire-EDM cutting method was used. It is worth mentioning here that the cut face and mirror cut face show some irregularity of distribution between peaks and valleys unlike their zone A performance. During machining of aluminum alloy 6060 using thin brass electrodes the highest material removal rate was witnessed. Wire brass as an electrode material does not allow the absorption of much heat energy because it has comparatively low thermal conductivity and most of the heat is consumed in the removal of material from a workpiece of the aluminum alloy 6060 at a small melting point.

Figure 8(d) shows the mean and standard deviation (mean±SD) values of the aluminum alloy 6060 cuts by wire-EDM including the cut face and mirror cut face at level 1 of the process parameters. As can be seen, the mean±SD values at level 1 (zone A) were 3.47±0.3 µm (for cut face) and 3.91±0.17 µm (for mirror cut face) indicating an 11.3% increase for the mirror cut face compared to cut face at the same spot of measurement with the same standard deviation. The mean±SD values at level 1 (zone B) were 3.56±0.25 µm (for cut face) and 3.69±0.21 µm (for mirror cut face) indicating a 3.5% increase for the mirror cut face compared to cut face at the same spot of measurement with 16% differences in the standard deviation. The mean±SD values at level 1 (zone C) were 3.29±0.11 µm (for cut face) and 3.71±0.41 µm (for mirror cut face) indicating a 11.3% increase for the mirror cut face compared to cut face at the same spot of measurement with 73% differences in the standard deviation. Roughly speaking, zone C (ending point) represents the smoothest average surface roughness compared with zone A (starting point) and zone B (middle point).

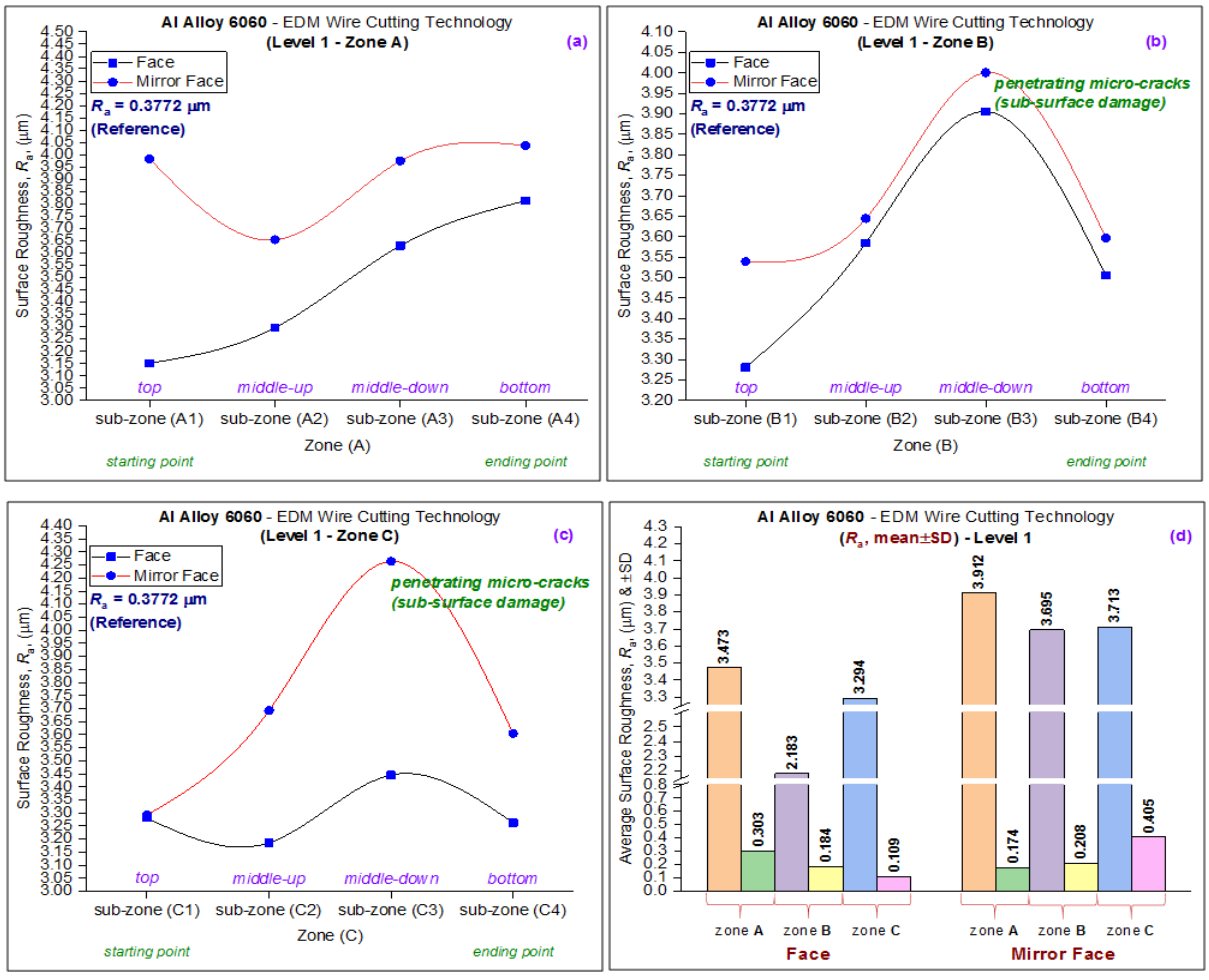

Figure 8. Surface roughness of aluminum alloy 6060 at level 1 parameters with different zones (a) zone A, (b) zone B, (c) zone C and (d) average surface roughness with a standard deviation

Figure 9(a), Figure 9(b) and Figure 9(c) show unpredicted behavior of the surface roughness performance of aluminum alloy 6060 (Al = 98.5%) cut by brass wire-EDM at level 2 process parameters (WFR = 5 mm/min) and measured at three different zones (A, B and C) and four different sub-zones (A1, A2, A3 and A4), (B1, B2, B3 and B4) and (C1, C2, C3 and C4) for both cut face and mirror cut face.

At level 2 (5 mm/min wire feed rate) and zone A, as shown in Figure 9(a), the surface roughness values of the cut face were increased from 3.71 µm (at the top area, sub-zone A1) until it reached 3.87 µm (at the bottom area, sub-zone A4), where the cutting has been done by a lateral cross-section of the target material whereas, the surface roughness values of the mirror cut face were dropped dramatically from 4 µm (at the top area, sub-zone A1) until it reached 3.8 µm (at the bottom area, sub-zone A4). This behavior indicates that there are some differences between the cut face and mirror cut face by almost ~0.13 µm implying smoother surface roughness in the former by almost 3.3%, although the same brass wire-EDM cutting method was used.

At level 2 (5 mm/min wire feed rate) and zone B, as shown in Figure 9(b), the surface roughness values of the cut face were increased from 3.94 µm (at the top area, sub-zone A1) until it reached 4.01 µm (at the bottom area, sub-zone B4), where the cutting has been done by a lateral cross-section of the target material whereas, the surface roughness values of the mirror cut face fluctuated between 3.65 µm to 3.93 µm all over subzones. This behavior indicates that there are some differences between the cut face and mirror cut face by almost ~0.02 µm implying smoother surface roughness in the former with rougher surface roughness by 0.5%, although the same brass wire-EDM cutting method was used. Another point worth mentioning is that the cut face and mirror cut face do not follow the same behavior and same trend of peaks and valleys as in their zone B performance.

At level 2 (5 mm/min wire feed rate) and zone C, as shown in Figure 9(c), the surface roughness values of the cut face were increased from 2.98 µm (at the top area, sub-zone C1) until they reached 4.05 µm (at the middle-up area, sub-zone C2) and then dropped to 3.38 µm, where the cutting has been done by a lateral cross-section of the target material. In contrast, the surface roughness values of the mirror cut face fluctuated between 3.33 µm to 3.92 µm. This behavior indicates that there are some differences between the cut face and mirror cut face by almost ~0.46 µm implying smoother surface roughness in the former, although the same brass wire-EDM cutting method was used. Another point worth mentioning is that the cut face and mirror cut face show some irregularity of distribution between peaks and valleys unlike their zone A performance.

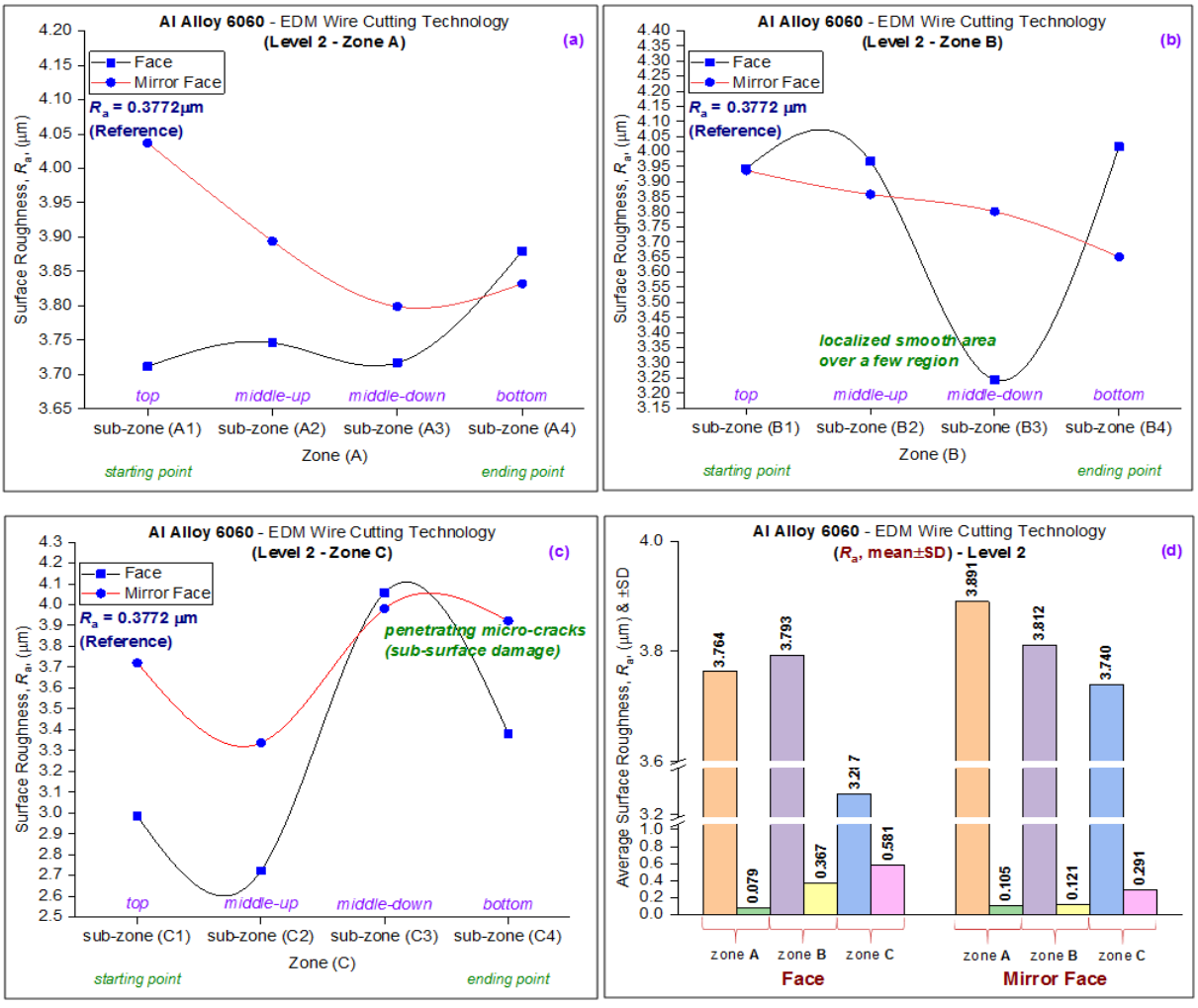

Figure 9. Surface roughness of aluminum alloy 6060 at level 2 parameters with different zones (a) zone A, (b) zone B, (c) zone C and (d) average surface roughness with a standard deviation

Figure 9(d) shows the mean and standard deviation (mean±SD) values of the carbon steel 1017 cut by wire-EDM including the cut face and mirror cut face at level 2 of the process parameters. As can be seen, the mean±SD values at level 2 (zone A) were 3.76±0.07 µm (for cut face) and 3.89±0.11 µm (for mirror cut face) indicating a 3.3% increase for the mirror cut face compared to cut face at the same spot of measurement with the same standard deviation. The mean±SD values at level 2 (zone B) were 3.79±0.36 µm (for cut face) and 3.81±0.12 µm (for mirror cut face) indicating a 0.5% increase for the mirror cut face compared to cut face at the same spot of measurement with 66% differences in the standard deviation. The mean±SD values at level 2 (zone C) were 3.28±0.58 µm (for cut face) and 3.74±0.29µm (for mirror cut face) indicating a 12.3% increase for the mirror cut face compared to cut face at the same spot of measurement with the 50% differences in the standard deviation. Overall, zone C (ending point) represents the smoothest average surface roughness compared with zone A (starting point) and zone B (middle point).

Figure 10(a), Figure 10(b) and Figure 10(c) show unpredicted behavior of the surface roughness performance of aluminum alloy 6060 (Al = 98.5%) cut by brass wire-EDM at level 3 process parameters (WFR = 7 mm/min) and measured at three different zones (A, B and C) and four different sub-zones (A1, A2, A3 and A4), (B1, B2, B3 and B4) and (C1, C2, C3 and C4) for both cut face and mirror cut face.

At level 3 (7 mm/min wire feed rate) and zone A, as shown in Figure 10(a), the surface roughness values of both cut face and mirror cut face fluctuated between 3.55 µm to 3.75 µm and 3.53 µm to 4.01 µm, respectively, where the cutting has been done by a lateral cross-section of the target material. This behavior indicates that there are some differences between the cut face and mirror cut face and irregularity distribution by almost ~0.04 µm implying smoother surface roughness in the former, although the same brass wire-EDM cutting method was used.

At level 3 (7 mm/min wire feed rate) and zone B, as shown in Figure 10(b), the surface roughness values of the cut face and mirror cut face follow the same patterns, that is, were increased from 3.62 µm and 3.42 µm (at the top area, sub-zone C1), respectively, until they reached 4.17 µm and 4.05 µm (at the middle-down area, sub-zone C3), respectively, and then dropped to 3.64 µm and 3.53 µm, respectively, where the cutting has been done by a lateral cross-section of the target material. This behavior indicates that there are some differences between the cut face and mirror cut face by almost ~0.12 µm implying smoother surface roughness in the later, although the same brass wire-EDM cutting method was used. It is absolutely worth mentioning here that the cut face and mirror cut face follow the same behavior and same trend of peaks and valleys unlike their zone A performance.

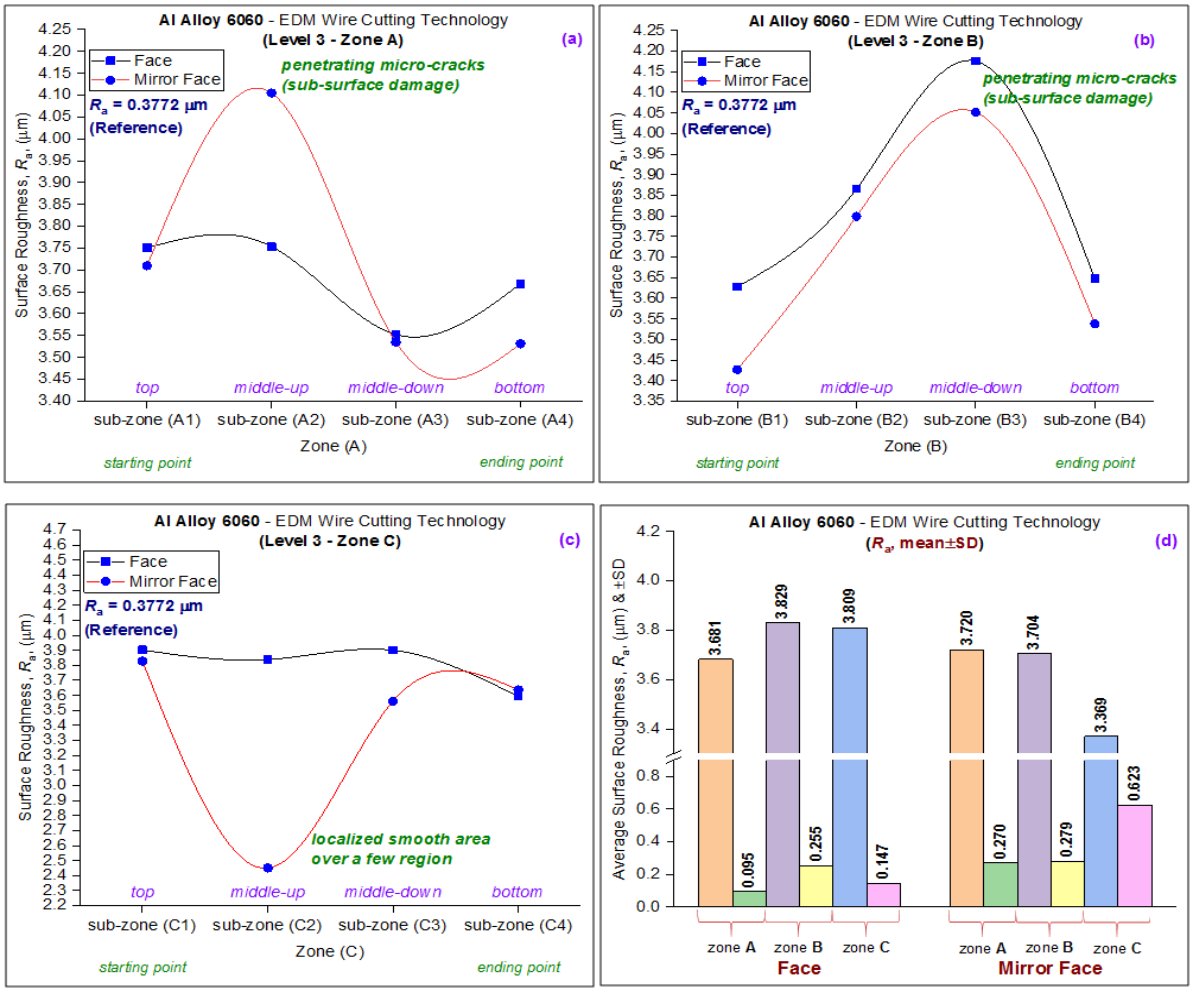

Figure 10. Surface roughness of aluminum alloy 6060 at level 3 parameters with different zones (a) zone A, (b) zone B, (c) zone C and (d) average surface roughness with a standard deviation

At level 3 (7 mm/min wire feed rate) and zone C, as shown in Figure 10(c), the surface roughness values of the cut face were almost constant at sub-zones C1, C2 and C3 by 3.9 µm and then dropped to 3.95 µm, where the cutting has been done by a lateral cross-section of the target material whereas, the surface roughness values of the mirror cut face play entirely different roles compared with the cut face. This behavior indicates that there are some differences between the cut face and mirror cut face by almost ~0.44 µm implying smoother surface roughness in the latter, although the same brass wire-EDM cutting method was used. It is absolutely worth mentioning that the cut face and mirror cut face show some irregularity distribution between peaks and valleys unlike their zone B performance.

Figure 10(d) shows the mean and standard deviation (mean±SD) values of the aluminum alloy 6060 cuts by wire-EDM including the cut face and mirror cut face at level 3 of the process parameters. As can be seen, the mean±SD values at level 3 (zone A) were 3.68±0.09 µm (for cut face) and 3.72±0.26 µm (for mirror cut face) indicating a 1.1% increase for the mirror cut face compared to cut face at the same spot of measurement with the 65% differences in the standard deviation. The mean±SD values at level 3 (zone B) were 3.82±0.25 µm (for cut face) and 3.7±0.27 µm (for mirror cut face) indicating a 3.1% decrease for the mirror cut face compared to cut face at the same spot of measurement with the 7% differences in the standard deviation. The mean±SD values at level 3 (zone C) were 3.81±0.14 µm (for cut face) and 3.37±0.62 µm (for mirror cut face) indicating a 11.6% decrease for the mirror cut face compared to cut face at the same spot of measurement with the 77% differences in the standard deviation. Roughly speaking, zone C (ending point) represents the smoothest average surface roughness compared with zones A and B (starting point and middle point).

In contrast with carbon steel 1017 (Fe = 98.4%), R_a decreased in aluminum alloy 6060 (Al = 98.5%) samples with increased wire feed rate and the best-achieved surface roughness was R_a = 2.44 µm (a better surface quality than carbon steel 1017) at a 7 mm/min wire feed rate (level 3) and with no striations all over the aluminum alloy 6060 samples. The surface roughness of aluminum alloy 6060 was increased compared to carbon steel 1017 samples due to the fact that the porosity found in aluminum alloy 6060 samples results in deeper cracks all over the profile. Hence, to obtain a good surface quality finish of a wire-EDM workpiece, it is desirable to set a low wire feed rate where stable machining without wire breakage becomes possible. As the wire feed rate increases, the consumption of wire will increase which consequently increases the machining cost. Low wire speed will cause wire breakage in high cutting speed. Along with the wire feed rate, pulse-on time and peak current should be set as low as possible (or pulse-off time should be set as high as possible). However, machining a material at low levels of these process parameters causes a lengthy machining time. More importantly, the surface roughness is directly dependent on the amount the target material solidifies on the machined surface.

4. Conclusions

In this paper, experimental investigation of the wire-EDM on both carbon steel 1017 (Fe = 98.4%) and aluminum alloy 6060 (Al = 98.5%) has been completed, and the following conclusions are drawn, based on the relationship between wire-EDM parameters and surface roughness, R_a:

- No striation pattern was observed from the top of the cut to the bottom of the cut for both target materials and both cut face and mirror cut face.
- Penetrating micro-cracks in the sub-surface and localized smooth area were observed over a few regions.
- The surface roughness behavior of the carbon steel 1017 (Fe = 98.4%) is better than that of aluminum alloy 6060 (Al = 98.5%) as it is an excellent conductor material.
- Aluminum alloy 6060 (Al = 98.5%) has higher thermal conductivity and low melting point causing substantial creator formation resulting in increases in the average surface roughness, R_a.
- The general trend observed indicates that the R_a quality improved and gives an excellent smooth surface with a reduction in the wire feed rate from 7 mm/min to 3 mm/min.
- Surface roughness was increased when the wire feed rate increased for both materials (carbon steel 1017 and aluminum alloy 6060). This indicates that the R_a of the wire-EDM workpiece is determined by the same machining variables, regardless of the material type being machined.
- Wire feed rate (WFR) is observed to have a significant role in the machining while considering the surface finish.
- Higher surface roughness is obtained for microscale surfaces mainly due to higher wear of the tool electrode and this may be one of the factors influencing irregular roughness.
- The cut face has always represented smooth surface roughness whereas the mirror cut face represents rough surface roughness for both machines' target materials.
- Zone C (ending point) represents the lowest R_a for carbon steel 1017 (Fe = 98.4%) for all three different levels of process parameters.
- Zone B (middle point) represents the lowest R_a for aluminum alloy 6060 (Al = 98.5%) for only level 1 process parameter (WFR = 3 mm/min) while level 2 and level 3 process parameters (WFR = 5 mm/min and 7 mm/min) go to zone C like carbon steel 1017.
- Overall, there is a bias between the cut face and mirror cut face for both target materials and different process parameter levels, although the same thin brass wire-EDM cutting method was used and the same cutting direction was carried out by a lateral cross-section of the target materials.

Conflicts of Interest

The authors have no conflicts of interest.

Funding Source

The authors received no financial support for the research and/or for the publication of this article.

Availability of Data and Materials

The data analyzed for this manuscript is the part of our research work and is available for public users.

References

[1] Salman, Ö. and M.C. Kayacan, *Evolutionary programming method for modeling the EDM parameters for roughness.* Journal of Materials Processing Technology, 2008. 200(1): p. 347-355.

[2] Kiyak, M. and O. Çakır, *Examination of machining parameters on surface roughness in EDM of tool steel.* Journal of Materials Processing Technology, 2007. 191(1): p. 141-144.

[3] Luis, C.J., I. Puertas, and G. Villa, *Material removal rate and electrode wear study on the EDM of silicon carbide.* Journal of Materials Processing Technology, 2005. 164-165: p. 889-896.

[4] Ho, K.H. and S.T. Newman, *State of the art electrical discharge machining (EDM).* International Journal of Machine Tools and Manufacture, 2003. 43(13): p. 1287-1300.

[5] Zeilmann, R.P., T. Ivaninski, and C. Webber, *Surface integrity of AISI H13 under different pulse time and depths by EDM process.* Procedia CIRP, 2018. 71: p. 472-477.

[6] Tilekar, S., S.S. Das, and P.K. Patowari, *Process Parameter Optimization of Wire EDM on Aluminum and Mild Steel by Using Taguchi Method.* Procedia Materials Science, 2014. 5: p. 2577-2584.

[7] Puertas, I., C.J. Luis, and G. Villa, *Spacing roughness parameters study on the EDM of silicon carbide.* Journal of Materials Processing Technology, 2005. 164-165: p. 1590-1596.

[8] Puertas, I. and C.J. Luis, *A study on the machining parameters optimisation of electrical discharge machining.* Journal of Materials Processing Technology, 2003. 143-144: p. 521-526.

[9] Klocke, F., et al., *Investigations on Surface Integrity of Heat Treated 42CrMo4 (AISI 4140) Processed by Sinking EDM.* Procedia CIRP, 2016. 42: p. 580-585.

[10] Kunieda, M., et al., *Advancing EDM through Fundamental Insight into the Process.* CIRP Annals, 2005. 54(2): p. 64-87.

[11] Schumacher, B.M., *After 60 years of EDM the discharge process remains still disputed.* Journal of Materials Processing Technology, 2004. 149(1): p. 376-381.

[12] Yin, Q., et al., *Research of lower tool electrode wear in simultaneous EDM and ECM.* Journal of Materials Processing Technology, 2014. 214(8): p. 1759-1768.

[13] Garg, R.K., et al., *Review of research work in sinking EDM and WEDM on metal matrix composite materials.* The International Journal of Advanced Manufacturing Technology, 2010. 50(5): p. 611-624.

[14] Srinivasa Rao, P., K. Ramji, and B. Satyanarayana, *Effect of wire EDM conditions on generation of residual stresses in machining of aluminum 2014 T6 alloy.* Alexandria Engineering Journal, 2016. 55(2): p. 1077-1084.

[15] Welling, D., *Results of Surface Integrity and Fatigue Study of Wire-EDM Compared to Broaching and Grinding for Demanding Jet Engine Components Made of Inconel 718.* Procedia CIRP, 2014. 13: p. 339-344.

[16] Bobbili, R., V. Madhu, and A.K. Gogia, *An experimental investigation of wire electrical discharge machining of hot-pressed boron carbide.* Defence Technology, 2015. 11(4): p. 344-349.

[17] Takayama, Y., et al., *The Latest Technology of Wire-cut EDM.* Procedia CIRP, 2016. 42: p. 623-626.

[18] Maradia, U., et al., *Electrode wear protection mechanism in meso–micro-EDM.* Journal of Materials Processing Technology, 2015. 223: p. 22-33.

[19] Fu, X., et al., *Surface Roughness Research of Piezoelectric Self adaptive Micro-EDM.* Procedia CIRP, 2016. 42: p. 563-568.

[20] Tsai, H.C., B.H. Yan, and F.Y. Huang, *EDM performance of Cr/Cu-based composite electrodes.* International Journal of Machine Tools and Manufacture, 2003. 43(3): p. 245-252.

[21] 2Ramarao, P.V. and M.A. Faruqi, *Characteristics of the surfaces obtained in electro-discharge machining.* Precision Engineering, 1982. 4(2): p. 111-113.

[22] Wang, C.C., et al., *Cutting austempered ductile iron using an EDM sinker.* Journal of Materials Processing Technology, 1999. 88(1): p. 83-89.

[23] Lee, S.H. and X.P. Li, *Study of the effect of machining parameters on the machining characteristics in electrical discharge machining of tungsten carbide.* Journal of Materials Processing Technology, 2001. 115(3): p. 344-358.

[24] Halkaci, H.S. and A. Erden. *Experimental investigation of surface roughness in electric discharge machining (EDM).* in *Proceedings of the 6th Biennial Conference on Engineering Systems Design and Analysis.* 2002. Istanbul, Turkey: ASME.

[25] Lee, S.H. and X. Li, *Study of the surface integrity of the machined workpiece in the EDM of tungsten carbide.* Journal of Materials Processing Technology, 2003. 139(1): p. 315-321.

[26] Guu, Y.H., et al., *Effect of electrical discharge machining on surface characteristics and machining damage of AISI D2 tool steel.* Materials Science and Engineering: A, 2003. 358(1): p. 37-43.

[27] Çoğun, C., B. Kocabaş, and A. Özgedik, *Experimental and theoretical investigation of workpiece surface profiles in electrical discharge machining (EDM)* Journal of the Faculty of Engineering and Architecture of Gazi University, 2004. 19(1): p. 97-106.

[28] Keskin, Y., H.S. Halkacı, and M. Kizil, *An experimental study for determination of the effects of machining parameters on surface roughness in electrical discharge machining (EDM).* The International Journal of Advanced Manufacturing Technology, 2006. 28(11): p. 1118-1121.

[29] Ozgedik, A. and C. Cogun, *An experimental investigation of tool wear in electric discharge machining.* The International Journal of Advanced Manufacturing Technology, 2006. 27(5): p. 488-500.

[30] Singh, S., S. Maheshwari, and P.C. Pandey, *Some investigations into the electric discharge machining of hardened tool steel using different electrode materials.* Journal of Materials Processing Technology, 2004. 149(1): p. 272-277.

[31] Singh, S. and A. Bhardwaj, *Review to EDM by Using Water and Powder-Mixed Dielectric Fluid.* Journal of Minerals and Materials Characterization and Engineering, 2011. 10(2): p. 199-230.

[32] Patel, V.D., et al., *Review of Wire-Cut EDM Process on Titanium alloy.* International Journal of Engineering Research and Applications 2014. 4(12): p. 112-121.

[33] Dong, W.P., P.J. Sullivan, and K.J. Stout, *Comprehensive study of parameters for characterizing three-dimensional surface topography I: Some inherent properties of parameter variation.* Wear, 1992. 159(2): p. 161-171.

[34] Dong, W.P., P.J. Sullivan, and K.J. Stout, *Comprehensive study of parameters for characterizing three-dimensional surface topography II: Statistical properties of parameter variation.* Wear, 1993. 167(1): p. 9-21.

[35] Dong, W.P., P.J. Sullivan, and K.J. Stout, *Comprehensive study of parameters for characterizing three-dimensional surface topography III: parameters for characterising amplitude and some functional properties.* Wear, 1994. 178(1): p. 29-43.

[36] Dong, W.P., P.J. Sullivan, and K.J. Stout, *Comprehensive study of parameters for characterising three-dimensional surface topography: IV: Parameters for characterising spatial and hybrid properties.* Wear, 1994. 178(1-2): p. 45-60.

[37] Thomas, T.R., *Characterization of surface roughness.* Precision Engineering, 1981. 3(2): p. 97-104.

[38] Alsoufi, M.S. and T.M. Bawazeer, *Quantifying assessment of touch-feel perception: an investigation using stylus base equipment and self-touch (human fingertip).* Umm Al-Qura University: Journal of Engineering and Architecture, 2015. 1(1): p. 1-16.

[39] Alsoufi, M.S. and T.M. Bawazeer, *The Effect of Aggressive Biological Materials on a Painted Automotive Body Surface Roughness.* American Journal of Nano Research and Applications, 2015. 3(2): p. 17-26.

[40] Suker, D.K., et al., *Studying the Effect of Cutting Conditions in Turning Process on Surface Roughness for Different Materials.* World Journal of Research and Review (WJRR) 2016 2(4): p. 16-21.

[41] Alsoufi, M.S., et al., *Experimental Study of Surface Roughness and Micro-Hardness Obtained by Cutting Carbon Steel with Abrasive WaterJet and Laser Beam Technologies.* American Journal of Mechanical Engineering, 2016. 4(5): p. 173-181.

[42] Bawazeer, T.M., et al., *Effect of Aqueous Extracts of Salvadora Persica "Miswak" on the Acid Eroded Enamel Surface at Nano-Mechanical Scale.* Materials Sciences and Applications, 2016. 7(11): p. 754-771.

[43] Alsoufi, M.S., et al., *Surface Roughness and Knoop Indentation Micro-Hardness Behavior of Aluminium Oxide (Al_2O_3) and Polystyrene ($C_8H_8)_n$ Materials* International Journal of Mechanical & Mechatronics Engineering 2016. 16(6): p. 43-49.

[44] Alsoufi, M.S., *State-of-the-Art in Abrasive Water Jet Cutting Technology and the Promise for Micro- and Nano-Machining.* International Journal of Mechanical Engineering and Applications, 2017. 5(1): p. 1-14.

[45] Alsoufi, M.S., et al., *Influence of Abrasive Waterjet Machining Parameters on the Surface Texture Quality of Carrara Marble.* Journal of Surface Engineered Materials and Advanced Technology, 2017. 7(2): p. 25-37.

[46] Alsoufi, M.S., et al., *Abrasive WaterJet Machining of Thick Carrara Marble: Cutting Performance vs. Profile, Lagging and WaterJet Angle Assessments.* Materials Sciences and Applications, 2017. 8(5): p. 361-375.

[47] Alsoufi, M.S., et al., *The Effect of Detergents on the Appearance of Automotive Clearcoat Systems Studied in an Outdoor Weathering Test* Materials Sciences and Applications, 2017. 8(7): p. 521-536.

[48] Alsoufi, M.S. and A.E. El-Sayed, *Warping Deformation of Desktop 3D Printed Parts Manufactured by Open Source Fused Deposition Modeling (FDM) System.* International Journal of Mechanical and Mechatronics Engineering, 2017. 17(4): p. 7-16.

[49] Alsoufi, M.S. and A.E. El-Sayed, *How Surface Roughness Performance of Printed Parts Manufactured by Desktop FDM 3D Printer with PLA+ is Influenced by Measuring Direction.* American Journal of Mechanical Engineering, 2017. 5(5): p. 211-222.

[50] Alsoufi, M.S. and A.E. El-Sayed, *Surface Roughness Quality and Dimensional Accuracy - A Comprehensive Analysis of 100% Infill Printed Parts Fabricated by a Personal/Desktop Cost-Effective FDM 3D Printer* Materials Sciences and Applications, 2018. 9(1): p. 11-40.

[51] Alsoufi, M.S. and A.E. El-Sayed, *Quantitative analysis of 0% infill density surface profile of printed part fabricated by personal FDM 3D printer* International Journal of Engineering & Technology, 2018. 7(1): p. 44-52.

[52] ISO4287, *Geometrical Product Specifications (GPS) -- Surface texture: Profile method -- Terms, definitions and surface texture parameters.* 1997, ISO.

[53] Wang, W., et al., *High efficiency slicing of low resistance silicon ingot by wire electrolytic-spark hybrid machining.* Journal of Materials Processing Technology, 2009. 209(7): p. 3149-3155.

[54] Punturat, J., V. Tangwarodomnukun, and C. Dumkum, *Surface characteristics and damage of monocrystalline silicon induced by wire-EDM.* Applied Surface Science, 2014. 320: p. 83-92.